

UCLA

UCLA Previously Published Works

Title

The joint effect of aging and HIV infection on microstructure of white matter bundles

Permalink

<https://escholarship.org/uc/item/51m5f8d1>

Journal

Human Brain Mapping, 40(15)

ISSN

1065-9471

Authors

Kuhn, Taylor
Jin, Yan
Huang, Chao
et al.

Publication Date

2019-10-15

DOI

10.1002/hbm.24708

Peer reviewed

RESEARCH ARTICLE

The joint effect of aging and HIV infection on microstructure of white matter bundles

Taylor Kuhn¹  | Yan Jin^{2,3} | Chao Huang³ | Yeun Kim⁴ | Talia M. Nir² | Joseph M. Gullett⁵ | Jacob D. Jones^{1,6} | Phillip Sayegh⁷ | Caroline Chung⁸ | Bianca H. Dang¹ | Elyse J. Singer¹ | David W. Shattuck⁴ | Neda Jahanshad² | Susan Y. Bookheimer¹ | Charles H. Hinkin¹ | Hongtu Zhu^{3,9} | Paul M. Thompson² | April D. Thames^{1,10}

¹Department of Psychiatry and Biobehavioral Sciences, University of California, Los Angeles, Los Angeles, California

²Imaging Genetics Center, Mark and Mary Stevens Neuroimaging and Informatics Institute, Keck School of Medicine, University of Southern California, Marina del Rey, California

³Department of Biostatistics, University of Texas MD Anderson Cancer Center, Houston, Texas

⁴Department of Neurology, University of California, Los Angeles, Los Angeles, California

⁵Center for Cognitive Aging and Memory, University of Florida, Gainesville, Florida

⁶Department of Psychology, California State University San Bernardino, San Bernardino, California

⁷Department of Psychology, University of California, Los Angeles, Los Angeles, California

⁸Department of Radiation Oncology, The University of Texas MD Anderson Cancer Center, Houston, Texas

⁹Department of Biostatistics, Gillings School of Global Public Health, University of North Carolina at Chapel Hill, Chapel Hill, North Carolina

¹⁰Department of Psychology, University of Southern California, Los Angeles, California

Correspondence

Taylor Kuhn, Ph.D., Department of Psychiatry and Biobehavioral Sciences, University of California, Los Angeles, Los Angeles, CA.
Email: tkuhn@mednet.ucla.edu

Funding information

Center for Scientific Review, Grant/Award Numbers: AG041915, EB20403, MH095661, MH19535, NS074980; UCLA Clinical and Translational Research Center, Grant/Award Numbers: UL1RR033176, UL1TR000124

Abstract

Recent evidence suggests the aging process is accelerated by HIV. Degradation of white matter (WM) has been independently associated with HIV and healthy aging. Thus, WM may be vulnerable to joint effects of HIV and aging. Diffusion-weighted imaging (DWI) was conducted with HIV-seropositive ($n = 72$) and HIV-seronegative ($n = 34$) adults. DWI data underwent tractography, which was parcellated into 18 WM tracts of interest (TOIs). Functional Analysis of Diffusion Tensor Tract Statistics (FADTTS) regression was conducted assessing the joint effect of advanced age and HIV on fractional anisotropy (FA), mean diffusivity (MD), axial diffusivity (AD), and radial diffusivity (RD) along TOI fibers. In addition to main effects of age and HIV on WM microstructure, the interactive effect of age and HIV was significantly related to lower FA and higher MD, AD, and RD across all TOIs. The location of findings was consistent with the clinical presentation of HIV-associated neurocognitive disorders. While older age is related to poorer WM microstructure, its detrimental effect on WM is stronger among HIV+ relative to HIV- individuals. Loss of WM integrity in the context of advancing age may place HIV+ individuals at increased risk for brain and cognitive compromise.

KEYWORDS

aging, DTI, HIV, tractography, white matter

1 | INTRODUCTION

Worldwide, ~37 million people are currently infected with HIV (HIV+). Of these, 5.8 (5.4–6.3) million are ages 50 years and older (Joint United Nations Programme on HIV/AIDS, 2016). As the HIV-infected population continues to age, understanding the synergistic effects of normal aging and HIV on brain microstructure is of ever-increasing importance. Prior neuroimaging studies showed HIV-associated degradation of the structural integrity of white matter (WM; Chang et al., 2008, 2011; Nir et al., 2014; Seider et al., 2016; Towgood et al., 2012; Wu et al., 2006), along with associated cognitive dysfunction (Chang et al., 2011), even in patients on effective antiretroviral therapies (Kuhn et al., 2018; Wu et al., 2006). Additionally, degradation of WM fibers is an established feature of the normal aging process (Gongvatana et al., 2011; Gunning-Dixon, Brickman, Cheng, & Alexopoulos, 2009; McWhinney, Tremblay, Chevalier, Lim, & Newman, 2016; Sexton et al., 2014; Westlye et al., 2010). However, the literature disagrees on whether there is an interactive relationship between HIV infection and aging in cognitively unimpaired patients (Holt, Kraft-Terry, & Chang, 2012).

Some scientists contend that there is no interactive or synergistic effect of HIV and aging on the brain (Cole et al., 2018; Valcour et al., 2004a), whereas others contend that HIV infection accelerates brain aging (Kuhn et al., 2016; Morgan, Lee, & Nyagode, 2011; Sacktor et al., 2010; Vance, McGuinness, Musgrove, Orel, & Fazeli, 2011). We suggest here that the previous inability to detect significant Age*HIV interactive effects in WM microstructure may be due to methodological differences (including neuroimage processing, statistical analysis, and sample size) rather than the lack of an Age*HIV interaction. Additionally, inconsistent reports may relate to biological differences across samples, including discrepancies in the degree of cognitive impairment and duration of infection. In fact, there is such variability in published diffusion tensor imaging (DTI) findings in HIV that this phenomenon has been studied and attributed, in part, to cohort selection (O'Connor, Jaillard, Renard, & Zeffiro, 2017). Therefore, the present study focused exclusively on cognitively unimpaired HIV+ participants.

In a cross-sectional DTI study, lower fractional anisotropy (FA) and higher axial diffusivity (AD), radial diffusivity (RD), and mean diffusivity (MD) were found pervasively throughout the entire WM, and most notably in the corpus callosum, superior corona radiata, and external capsule in a sample of older HIV+ participants compared to controls (Nir et al., 2014). A 1-year longitudinal study of cognitively unimpaired HIV+ participants showed higher diffusivity in the genu of the corpus callosum relative to baseline compared to controls. Further, the HIV group showed, on average, significantly higher MD changes in the frontal and parietal WM, putamen, and genu compared to baseline measures (Chang et al., 2008). However, these authors did not detect an interactive effect of HIV infection and age on WM. These authors also reported independent effects of age on FA, AD, RD, and MD throughout the brain. Again, this study did not find a significant interaction between HIV and age on WM microstructure, although this may be due

in part to the restricted, older age range of the studied cohort and the available sample size (i.e., 39 HIV+ participants).

Conversely, one recent study did report an interactive effect of HIV and age on both WM hyperintensities and FA in an HIV+ sample ($n = 88$) that remained when evaluating a subsample ($n = 43$) without Hepatitis C virus (HCV) coinfection and detectable HIV RNA (Seider et al., 2016). Similarly, some magnetic resonance spectroscopy (MRS) studies reported significant Age*HIV interactive effects, particularly for neurometabolites in the frontal WM (Cysique et al., 2013; Ernst & Chang, 2004; Harezlak et al., 2011). Therefore, there may be an interactive, or simply additive, effect of the HIV disease process and aging on brain structure. Although no studies to our knowledge have reported an interaction of HIV infection and age on WM microstructure in larger, solely monoinfected (i.e., no HCV) HIV+ cohorts, possibly due to cohort effects and/or insufficient spatial sensitivity of the analytic methods employed, recent machine learning studies have demonstrated an augmented or accentuated aging process in gray and WM volume (Cole et al., 2018; Cole, Caan, et al., 2018) and WM microstructure (Kuhn et al., 2018) with associated cognitive deficits.

One technique that can address such limitations from prior studies associated with insufficient spatial sensitivity of analytic methods is automated Multi-Atlas Tract Extraction procedure (*autoMATE* Jin et al., 2017), which is a highly spatially sensitive 3D tractography technique that allows for the investigation of WM microstructure along individual WM tracts (Jin et al., 2014, 2017). This method has previously been used to highlight the spatial distribution of neurodegenerative effects related to Alzheimer's disease (Jin, Shi, Zhan, & Thompson, 2015) and frontotemporal dementia (Daianu et al., 2016). While some prior HIV studies used voxel-wise analyses to investigate effects of HIV and age on WM (Chang et al., 2011; Nir et al., 2014; Seider et al., 2016), these analyses yield results along a single central line assumed to represent the entirety of a WM tract. Conversely, by using deterministic tractography to compute large-scale, multiple-fiber representations of WM tracts, *autoMATE* can better localize effects to specific regions of tracts, providing information on regionally specific changes in WM. To the best of our knowledge, no prior studies have used this 3D tractography technique to investigate changes related to disease or age in HIV (Jin et al., 2014). Thus, we examined the effects of HIV infection, age, and the interaction between HIV and age on WM microstructure along the length of fibers comprising several robustly identifiable WM tracts. Further, a past review suggested that aging effects in HIV may be limited to individuals with severe cognitive impairment (O'Connor et al., 2017); therefore, to limit this possible confound, we recruited a cognitively unimpaired sample with a wide age range (HIV+: 24–76 years; HIV–: 21–66 years), along with well-matched controls.

2 | MATERIALS AND METHODS

2.1 | Participants

Participants included 72 HIV+ (confirmed by serologic testing) and 32 HIV– participants who were enrolled as part of a larger study (K23

MH095661; PI: A.D.T.). All procedures were in accordance with the Declaration of Helsinki, reviewed and approved by the University of California, Los Angeles (UCLA) Institutional Review Board prior to enrollment. All participants provided written informed consent. The Structured Clinical Interview for DSM-IV (SCID-IV; First, Spitzer, Gibbon, & Williams, 1997) and questionnaires about neurological and other medical history were used to screen for neurological, psychiatric, and medical confounds, including: history of seizure disorder or other neurologic disorder; history of concussion or traumatic brain injury sufficient to warrant medical attention; history of Axis I psychiatric disorder or substance use disorder (SCID-IV diagnostic criteria); current prescription for psychotropic medication, except for anxiolytics and antidepressants; current substance use disorder or methamphetamine use; past opioid or stimulant use disorder; comorbid central nervous system (CNS) infection (e.g., HCV); and HIV-associated CNS opportunistic infection (e.g., toxoplasmosis) or neoplasm. A comprehensive neuropsychological evaluation involving empirical assessment of domain-level and global cognition was performed to ensure all participants were cognitively unimpaired. Cognitive impairment was operationalized as performance 1.0 standard deviations or more below the mean, based on published normative data, in two cognitive domains (Antinori et al., 2007). Participants were also screened for MRI contraindications.

2.2 | Group demographic comparison

Demographic factors (e.g., age and education [years]) and clinical factors (e.g., past drug use) between HIV+ and HIV- groups were compared using one-way analysis of variance (ANOVA). Group differences in dichotomous factors (e.g., sex, ethnicity, and urinalysis results) were assessed using chi-squared (χ^2) analyses. We used $p < .05$ as our cut-off for statistical significance for these demographic analyses.

2.3 | Neuroimaging acquisition

Diffusion-weighted imaging (DWI) and T1-anatomical scans were collected from HIV+ individuals ($n = 72$) ages 24–76 years and HIV- ($n = 34$) controls ranging in age from 21 to 66 years. DWI images consisted of 65 diffusion-weighted volumes ($b = 1,000$ s/mm²) and six nondiffusion-weighted ($b = 0$) volumes. All MRI data were collected using a 3 T Siemens Trio scanner (Siemens, Germany) located at the UCLA Center for Cognitive Neuroscience (CCN, Los Angeles, CA). DWI scans were collected using single-shot spin-echo planar imaging (EPI) with 60×2.0 mm axial slices (no gap), FOV = 190 mm (AP) \times 190 mm (RL), matrix = 190×190 , TR = 9,000 ms, TE = 93 ms, voxel size = $2.0 \times 2.0 \times 2.0$ mm, and b-shells = 0, 1,000. The acquisition time was 7 min and 16 s. T1-weighted anatomic scans were collected using a 12-channel head coil on Siemens Tim Trio 3 T scanner (Siemens Medical Solution, Erlangen, Germany) at the UCLA CCN. Structural MP-RAGE T1-weighted scans were acquired with 120 1.0-mm sagittal slices, FOV = 256 mm (AP) \times 192 mm (FH), matrix = 256×192 , TR = 450 ms, TE = 10 ms, Flip Angle = 8°, and

voxel size = $1.0 \times 0.94 \times 0.94$ mm. All images were quality controlled and visually inspected prior to being preprocessed and analyzed.

2.4 | Neuroimaging processing and analysis

The diffusion MRI data for each subject was first corrected for geometric distortion due to B0 inhomogeneity using the INVERSION (Bhushan et al., 2015) method implemented in BrainSuite version 16a (<http://brainsuite.org>). This process performs a constrained nonrigid registration between the subject's T1-weighted MRI and diffusion MRI data. The diffusion MRI data were then resampled to the coordinate space of the T1-weighted MRI using the estimated deformation field. Prior to distortion correction, each T1-weighted MRI was skull-stripped and corrected for nonuniformity using BSE and BFC, respectively (Shattuck, Sandor-Leahy, Schaper, Rottenberg, & Leahy, 2001); skull-stripping masks were manually corrected for four participants. Following a routine DWI processing pipeline carried out using FSL version 6.0 (Smith et al., 2004) involving brain extraction, correction for motion and eddy current distortion, and tensor-fitting, whole-brain tractography was conducted using Camino (<http://cmic.cs.ucl.ac.uk/camino/>). We then performed *autoMATE* (Jin et al., 2017) to parcellate and cluster 18 WM tracts of interest (TOIs) based on the Johns Hopkins University White Matter Atlas (Mori et al., 2008). *autoMATE* involves a harmonized, multi-atlas anatomical labelling approach that has been shown to outperform alternative single-atlas approaches (Doshi et al., 2016; Erus et al., 2018). Eighteen fiber TOIs were extracted from a previously constructed WM atlas (Mori et al., 2008). From each TOI, five manually labeled tracts were made based on tractography results from five healthy participants to create accurate models of these tracts in vivo. These manually labeled tracts were then warped to each subject's whole-brain tractography. For each manually labeled atlas, an automated clustering algorithm generated five individual cluster results for each TOI in each individual. These clusters were based on the warped overlap between each participant's WM fiber tracts and each manually labeled atlas. A fusion scheme then combined these five-clustered tracts into a single, final TOI for each participant. TOIs included: the bilateral anterior thalamic radiation (ATR; left = 652 fibers; right = 659 fibers), bilateral corticospinal tract (CST; left = 426 fibers, right = 437 fibers), bilateral inferior fronto-occipital fasciculi (IFO; left = 631 fibers, right = 571 fibers), bilateral inferior longitudinal fasciculus (ILF; left = 389 fibers, right = 254 fibers), fornix (FNX; 174 fibers), bilateral cingulate bundle (CGC; left = 400 fibers, right = 439 fibers), left arcuate fasciculus (ARC; 489 fibers), and corpus callosum (CC) fibers projecting to post-central gyrus (CC-POC; 237 fibers), precentral gyrus (CC-PRC; 401 fibers), frontal lobe (CC-FRN; 1,822 fibers), parietal lobe (CC-PAR; 616 fibers), temporal lobe (CC-TEM; 132 fibers), and occipital lobe (CC-OCC; 558 fibers). This process allowed us to generate high-confidence, anatomically plausible WM tracts for each participant.

For group-wise analyses, a fiber-matching scheme was used to register the tracts across the participant population (Westlye et al., 2010). The registered WM tracts resulted in data for each fiber in each tract in the same location for each participant. Each fiber was

then segmented into 25 equidistant sections onto which FA, MD, RD, and AD values were interpolated and used for statistical analysis. For a thorough review of these methods, please see Jin et al. (2017). Diffusion metrics were then statistically interrogated at each of the 25 points along every fiber within each tract using Functional Analysis of Diffusion Tensor Tract Statistics (FADTTS; Zhu et al., 2011). To demonstrate the spatial specificity of our results, Figures 1–3 are presented showing the distribution of significant results across WM tracts. The six WM tracts with the largest percentage (i.e., based on the number of points along the WM tract with significant findings divided by the total number of points along that WM tract) of significant results are shown for each analysis. The color bars correspond to the $-\log_{10} p$ -values.

While routine linear regression could be used to statistically interrogate this data, we chose to use an alternative approach that is optimized for statistics conducted on data with a spatial component. FADTTS regressions are similar to traditional regressions with a primary and important distinction that makes them well suited for DTI analysis: FADTTS regressions do not treat each data point (i.e., each point along a WM tract) as an independent observation. Instead, FADTTS regressions assume there is some shared variance among

neighboring data points, taking into account smoothness and spatial correlation between the neighboring points along each fiber and treating diffusion parameters as functions of their fiber locations. By acknowledging this dependence, or covariance, among neighboring points, these data points are treated as nonindependent, subsequently increasing statistical power. As such, FADTTS regressions may outperform traditional GLM analyses. Therefore, FADTTS regressions were applied to assess the independent (i.e., age and HIV-serostatus) and joint (interaction) effects of advanced age and HIV infection on FA, AD, RD, and MD at each point within each TOI fiber. This approach resulted in a unique analysis for each TOI.

The FADTTS regression treated each TOI as an independent region orthogonal to each other TOI. Thus, no correlation between TOIs was considered in the model. Within each TOI, each fiber was also treated as orthogonal to every other fiber within that region of interest. Therefore, no between-fiber correlations were included in the model. Conversely, within each fiber within each TOI, correlations were modeled between each of the 25 segments of individual fibers that were statistically interrogated. This intrafiber correlation was addressed in the FADTTS model using a stochastic variable that accounted for the covariance between the variables of interest

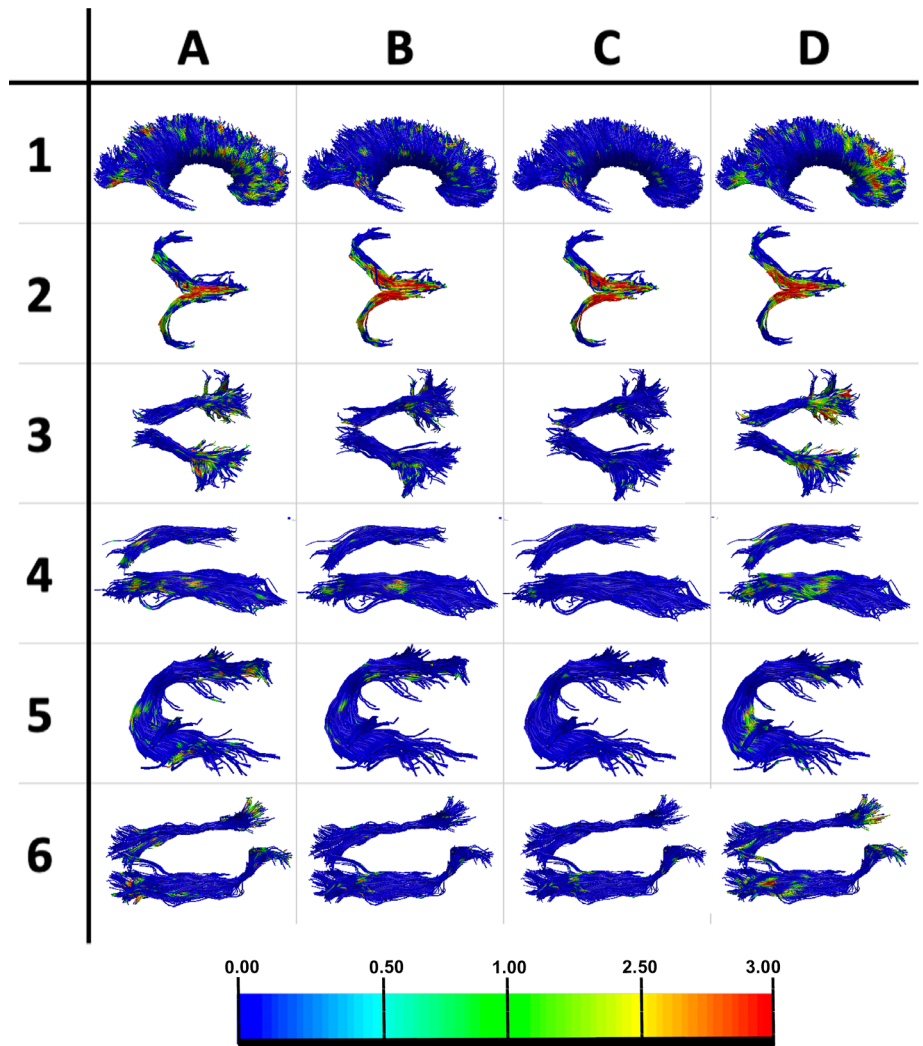


FIGURE 1 Depicting effect of advancing age on the CC (1), bilateral FRX (2), bilateral ATR (3), ILF (4), left ARC (5), and IFO (6) lower fractional anisotropy (a), and higher mean (b), axial (c), and radial diffusivity (d). The color bars correspond to the $-\log_{10} p$ -values, where statistical significance was denoted as all $-\log$ values > 1.3 ($p = .05$), after multiple comparisons correction was applied across all fibers using false discovery rate [Color figure can be viewed at wileyonlinelibrary.com]

(e.g., age) and two fibers points based on the physical distance between those two points. Sex, ethnicity, education (years), and participant self-reported nadir CD4 count and highest lifetime HIV viral load were included in the model as covariates. To remove effects of multicollinearity, the main effects of age and HIV status were controlled for when assessing the interactive effect of age and HIV serostatus. All statistical analyses, including within fibers, across fibers, and across TOIs, were corrected using the false discovery rate (FDR) method (Benjamini & Hochberg, 1995; Schwartzman, Dougherty, Lee, Ghahremani, & Taylor, 2009), with statistical significance denoted as the *P*-value threshold adjusted to correct for multiple comparisons (FDR at 5% [$q < 0.05$]). The percentages of fiber points that yielded significant results for each statistical analysis are presented in Tables 2–4 to help elucidate the spatial extent of the significant findings. For the tables as well as Figures 1–3, a percentage of the significant results of each variable of interest (e.g., main effect of age and interaction effect of Age*HIV) on each TOI was computed as: Number of points within the TOI where a significant effect was found \div Total number of points within that TOI.

3 | RESULTS

3.1 | Demographic group comparison

The HIV+ and HIV– groups did not differ significantly in age, years of education, ethnicity, or sex (all *p* values $>.10$). Nevertheless, given the fact that the distribution of male and female participants was qualitatively different between groups, and it is possible that hemispheric asymmetries in WM exist across sexes, sex was included as a covariate in the FADTTS model. None of the participants tested positive for barbiturates, cocaine, methamphetamine, phencyclidine, or MDMA. Significantly more HIV+ participants tested positive for prescribed benzodiazepines ($\chi^2 = 5.93$, $p = .015$) than HIV– participants. Although the groups did not statistically differ on current marijuana use, 11 (39.3%) controls and 24 (35.3%) HIV+ participants tested positive for marijuana on urinalysis. The HIV serostatus groups also did not differ on current alcohol or substance use or past substance use disorder status. Table 1 provides additional detail on group demographics.

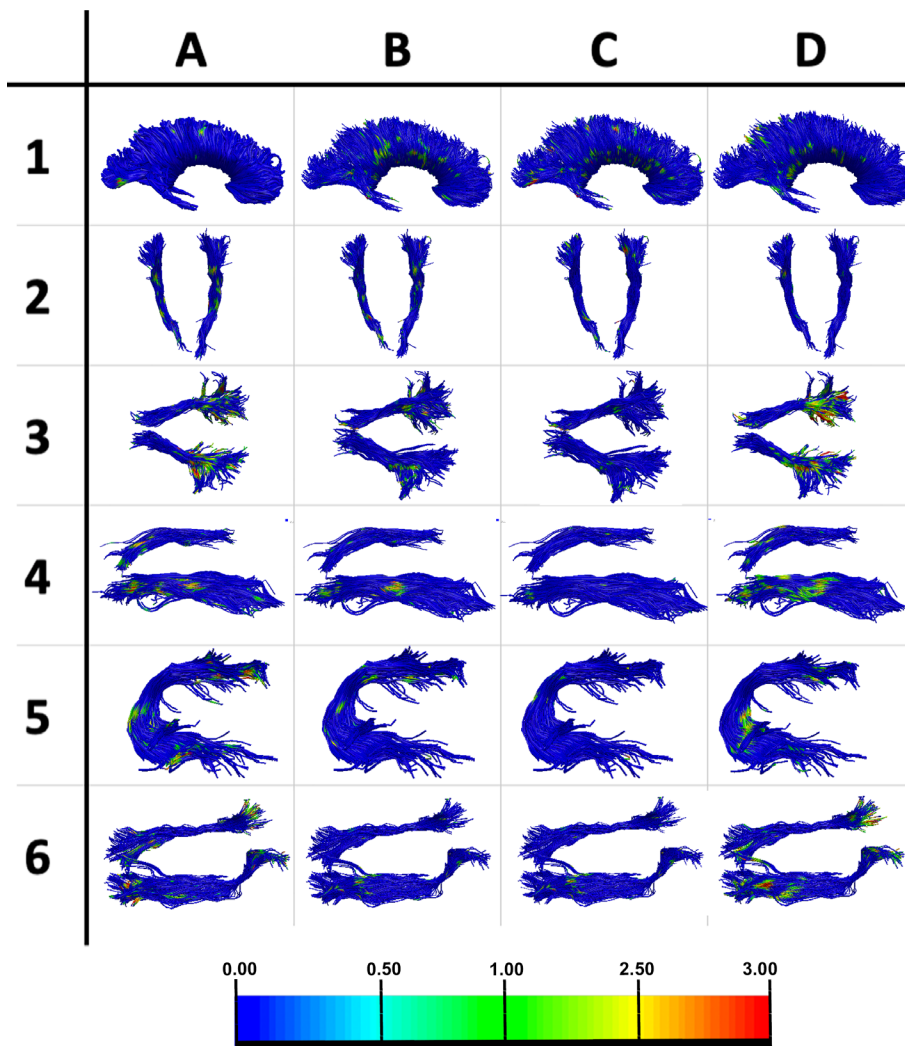
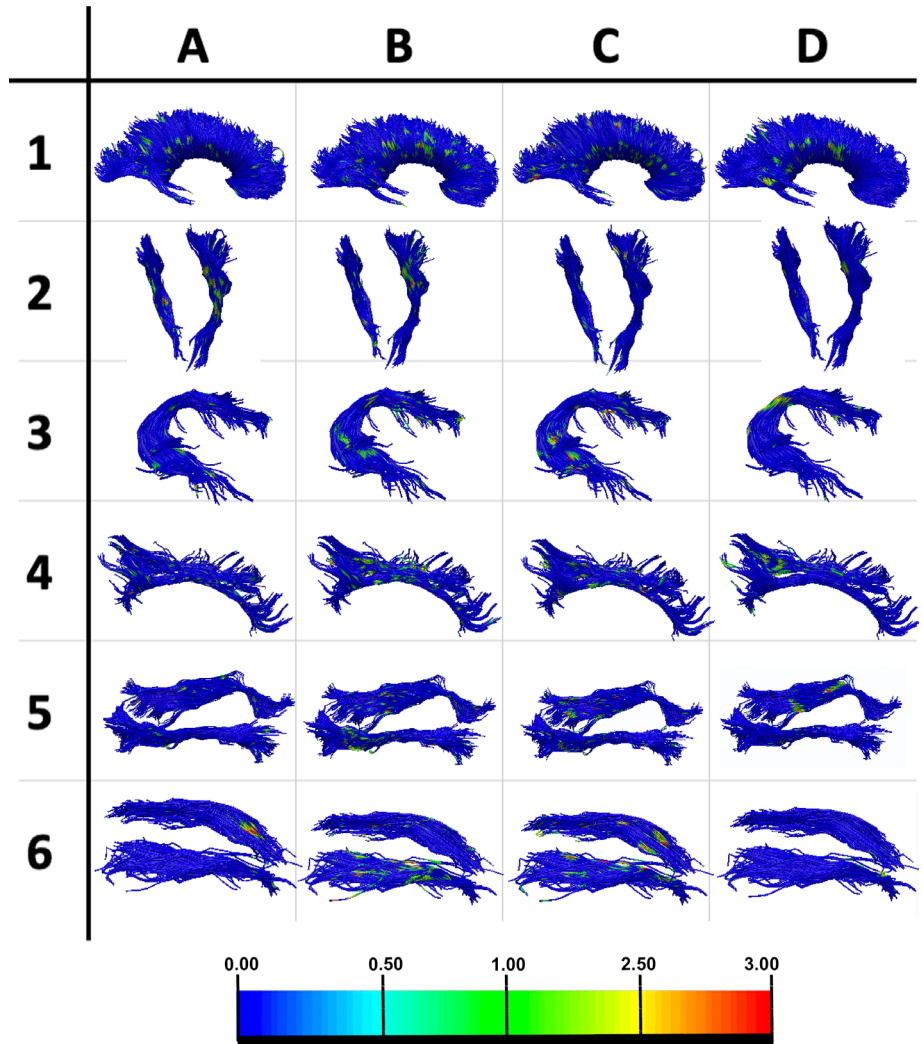


FIGURE 2 Depicting effect of HIV group status on the CC (1), bilateral CST (2), bilateral CGC (3), left ARC (4), ILF (5), and IFO (6). The HIV+ group evidenced higher fractional anisotropy (a), and lower me/an (b), axial (c), and radial diffusivity (d). The color bars correspond to the $-\log_{10} p$ -values, where statistical significance was denoted as all $-\log$ values >1.3 ($p = .05$), after multiple comparisons correction was applied across all fibers using false discovery rate [Color figure can be viewed at wileyonlinelibrary.com]

FIGURE 3 Depicting interactive effect of HIV infection and advancing age on the CC (1), bilateral CST (2), left ARC (3), bilateral CGC (4), ILF (5), and IFO (6) lower fractional anisotropy (a), and higher mean (b), axial (c), and radial diffusivity (d). The color bars correspond to the $-\log_{10} p$ -values, where statistical significance was denoted as all $-\log$ values > 1.3 ($p = .05$), after multiple comparisons correction was applied across all fibers using false discovery rate [Color figure can be viewed at wileyonlinelibrary.com]



3.2 | 3D Tractography analysis results

A significant main effect of age on WM was found, indicating that as age increased, there were significant FA decreases and MD, AD, and RD increases in all TOIs investigated (Table 2), all of which typically reflect poorer or more impacted WM microstructure. This effect of advancing age on WM microstructure was most pronounced in the CC-FRN, body and fimbria of the FNx, bilateral ATR fibers projecting to the frontal lobe, temporal portions of the ILF, language-dominant cortical projections from the ARC, and primarily frontal cortex projections from bilateral IFO (Figure 1).

Significant main effects of HIV serostatus were also found in all TOIs. Regions with reduced FA associated with HIV infection were found in the left ARC, left ATR, left CC-OCC, left IFO, and left ILF, as well as increased RD in the bilateral ATR, right CST, CC-FRN, right CGC, right IFO, and right ILF. However, the control group had significantly lower FA and higher diffusivity metrics in portions of all TOIs investigated compared to the HIV+ group (Table 3). These findings were more prominent across larger regions of TOIs and included the CC-TEM, CC-PAR, internal capsule and distal CST fibers, retrosplenial CGC, posterior ARC fibers, and medial regions of both ILF and IFO.

Regarding our key analysis pertaining to the joint effects of age and HIV on WM, measures of WM microstructure (i.e., FA, MD, RD, and AD) showed significant interactive effects of age and HIV status ($q < 0.05$). Specifically, the interaction effect revealed that measures that typically reflect poorer or more impacted WM microstructure (i.e., lower FA and higher MD, RD, and AD) were related to older age, and this effect was greater in HIV+ participants relative to HIV- participants. The interactive effect of HIV and advancing age was significantly related to lower FA, higher MD, higher AD, and higher RD across the regions of the CC, FNx, left AF, and bilateral ATR, CST, ILF, IFOF, and CB. When ranking TOIs based on the severity of the FA decrease with age, the interactive effect was most pronounced in the bilateral internal capsule (within the CST) and CC, particularly CC-TEM and CC-PAR (Figure 3). Interestingly, when ranking TOIs based on the severity of the AD increase with age, the interactive effect was strongest in the CC-TEM, the ARC fibers nearest language-involved cortex, posterior CGC regions, primarily temporal portions of bilateral ILF, internal capsule, portions of bilateral CST, and primarily frontal cortex projections from the right IFO.

Table 4 reports the percentage of points within each TOI where the interaction of HIV and age was significantly associated with DTI

TABLE 1 Demographic comparison between HIV+ and HIV– groups

	n = 72	n = 34
Demographic variable	HIV+	HIV–
Male sex (%)	58 (83%)	17 (50%)
Education (years)	13.32 ± 1.93	14.00 ± 2.56
Age (years)	50.7 ± 11.93	53.25 ± 10.28
Age range (years)	24–76	21–66
Ethnicity ^a	35% C, 65% AA	50% C, 50% AA
HIV duration	16.37 ± 8.13	
Pre-HAART ^b diagnosis	32 (46%)	
Nadir CD4 (#/mm ³)	246.1 ± 212.26	
Current CD4 (#/mm ³)	663.61 ± 282.426	
# (%) with detectable viral load	8 (11%)	
Peak viral load (IU/mL)	395,055.97 ± 767,296.72	
Current viral load (IU/mL)	13,571.19 ± 76,016.07	
(%) with major depression (SCID)	4 (7%)	1 (5%)
# (%), range in joints/day currently using marijuana	16 (22%, 1–3)	5 (16%, 1–5)
# (%), range in drinks/day currently using alcohol	31 (43%, 1–7)	18 (53%, 1–4)

$p < .05$.

^aAA, African American; C, Caucasian.

^bHAART, highly active antiretroviral therapy.

metric values. Simple effects post hoc analyses revealed that the negative effect of age on WM was significantly steeper ($q < 0.05$) in the HIV+ participants compared to their seronegative counterparts, indicating that the detrimental effect of aging on WM degradation is significantly stronger among HIV+ relative to HIV– individuals.

4 | DISCUSSION

This study examined the independent and interactive effects of age and HIV serostatus on microstructural measures from the major WM fiber bundles by using an automated clustering 3D tractography technique (*autoMATE* Jin et al., 2017). This neuroimaging analysis method offers a more localized measurement of 3D profiles of WM tracts than analyses conducted using a global metric of mean WM microstructure.

Although the presence of a significant Age*HIV interaction effect limits the interpretability of significant main effects, age and HIV infection were both found to independently relate to WM deterioration. As anticipated, significant effects of advancing age on WM microstructure were found, indicating that as age progresses, WM microstructure evidences deleterious changes. These findings are in line with a large extant literature (Cole, Ritchie, et al., 2018; Gongvatana et al., 2011;

TABLE 2 Effects of advancing age on white matter microstructure diffusivity values

Tract	FA–	MD+	AD+	RD+
CC-FRN	30.87	9.72	1.41	37.06
CC-OCC	5.81	2.3	1.43	8.72
CC-PAR	4.19	1.12	0.95	4.06
CC-POCG	10.9	2.73	0.39	6.11
CC-PRCG	18.7	6.99	0.94	10.16
CC-TEM	5.24	8.79	7.48	4.15
FNX	28.21	55.82	54.3	39.17
L-ARC	12.87	4.88	6.12	8.18
L-ATR	18.26	5.13	2.32	26.64
L-CGC	7.49	0.71	0.14	5.57
L-CST	3.31	1.31	0.91	2.36
L-IFO	13.19	3.96	1.71	11.01
L-ILF	18.52	4.14	0.85	12.53
R-ATR	19.5	7.85	3.37	14.28
R-CGC	8.31	1.18	1.5	2.33
R-CST	3.93	1.43	0.62	7.09
R-IFO	6.67	1.67	0.61	6.25
R-ILF	9.87	1.75	0.44	5.43

Values represent percent of entire tract where main effect of age was statistically significant after multiple comparison correction (FDR; $q < 0.05$). TOIs investigated: the bilateral anterior thalamic radiation (ATR), bilateral corticospinal tract (CST), bilateral inferior fronto-occipital fasciculi (IFO), bilateral inferior longitudinal fasciculus (ILF), fornix (FNX), bilateral cingulate bundle (CGC), left arcuate fasciculus (ARC), and corpus callosum (CC) fibers projecting to postcentral gyrus (CC-POC), precentral gyrus (CC-PRC), frontal lobe (CC-FRN), parietal lobe (CC-PAR), temporal lobe (CC-TEM), and occipital lobe (CC-OCC).

Gunning-Dixon et al., 2009; McWhinney et al., 2016; Sexton et al., 2014; Westlye et al., 2010) and are congruent with the neuropsychological changes associated with advanced aging (Pomara, Crandall, Choi, Johnson, & Lim, 2001; Summers & Bondi, 2017). Similarly, as expected and consistent with a larger literature (e.g., (Chang et al., 2011; Filippi, Uluğ, Ryan, Ferrando & van Gorp, 2001; Pomara et al., 2001; Seider et al., 2016; Wang et al., 2011; Wright, Heaps, Shimony, Thomas & Ances, 2012)), a significant main effect of HIV was found on WM. However, some TOIs evidenced WM deterioration that was greater in the seronegative control group, which may be explained by the heterogeneous nature of the cellular effect of HIV infection on WM. However, these simple main effects of age and HIV serostatus must be interpreted in light of an interaction effect. Specifically, when controlling for several potentially confounding factors (i.e., sex, ethnicity, education [years], nadir CD4 count, and highest lifetime HIV viral load), our key analyses revealed significant Age*HIV interactive effects in all TOIs. These results indicate that in addition to older age being related to poorer WM microstructural integrity, the detrimental effect of aging on WM is significantly stronger among HIV+ individuals relative to HIV– individuals. In several TOIs, including the CC, ILF, IFO, and ATR, interactive effects were strongest in fibers projecting to the

TABLE 3 Effect of HIV on white matter microstructure diffusivity values

Tract	FA–	MD+	AD+	RD+	FA+	MD–	AD–	RD–
CC-FRN	0.46	0.18	0.35	5.76	1.49	4.62	5.63	1.29
CC-OCC	1.00	0.24	0.52	0.38	4.36	6.95	6.34	10.02
CC-PAR	0.05	0.01	0.38	0	7.45	9.45	5.92	22.05
CC-POCG	0.95	0.03	0.91	0.05	3.51	4.35	6.58	9.37
CC-PRCG	0.4	0.02	0.28	0.84	1.89	2.02	4.85	2.47
CC-TEM	0.12	0.03	0.12	0.33	10.36	15.03	13.73	12.55
FNX	0.23	1.01	2.09	1.17	6.37	3.63	3.13	6.25
L-ARC	1.42	0.32	0.44	0.38	3	6.94	12.42	7.08
L-ATR	1.31	0.17	0.21	1.86	1.88	3.23	6.99	0.29
L-CGC	0.61	0.02	0.72	0.17	2.97	7.79	5.14	1.69
L-CST	0.62	0.18	0.6	0.4	8.36	5.92	3.16	1.58
L-IFO	1.01	0.61	0.39	0.72	3.39	4.66	4.2	7.27
L-ILF	1.71	0.68	0.57	0.15	2.4	3.77	6.01	5.15
R-ATR	0.41	0.01	0.15	6.27	3.09	5.34	6.79	2.01
R-CGC	0.54	0.05	0.23	1.07	6.24	15.54	6.56	22.54
R-CST	0.69	0.06	0.07	1.35	11.09	6.92	4.02	2.44
R-IFO	0.46	0.11	0.13	1.22	3.99	10.56	6.75	7.19
R-ILF	0.96	0.08	0.05	1.29	6.8	11.62	8.33	8

Values represent percent of entire tract where main effect of HIV was statistically significant after multiple comparison correction (FDR; $q < 0.05$). TOIs investigated: the bilateral anterior thalamic radiation (ATR), bilateral corticospinal tract (CST), bilateral inferior fronto-occipital fasciculi (IFO), bilateral inferior longitudinal fasciculus (ILF), fornix (FNX), bilateral cingulate bundle (CGC), left arcuate fasciculus (ARC), and corpus callosum (CC) fibers projecting to postcentral gyrus (CC-POC), precentral gyrus (CC-PRC), frontal lobe (CC-FRN), parietal lobe (CC-PAR), temporal lobe (CC-TEM), and occipital lobe (CC-OCC).

frontal and temporal lobes, consistent with knowledge of a relatively heterogeneous yet typically predominantly frontal-subcortical involvement in HIV (Ettenhofer & Abeles, 2009; Gullett et al., 2018; Heaton et al., 2010; Hinkin, Castellon, Atkinson, & Goodkin, 2001; Price, Bartlett, & Bloom, 2016; Valcour et al., 2004a; Valcour, Sithinamsuwan, Letendre, & Ances, 2011). These findings are also consistent with MRS studies that reported significant Age*HIV interactive effects, particularly for frontal WM metabolites (Cysique et al., 2013; Ernst & Chang, 2004; Harezlak et al., 2011); Age*HIV interactive effects were also reported in subcortical regions (Kuhn et al., 2018). Together, these findings both support and expand upon prior literature demonstrating jointly deleterious effects of HIV and aging on WM microstructure (Gullett et al., 2018; Holt et al., 2012; Nir et al., 2014; Towgood et al., 2012).

Importantly, prior failures to detect Age*HIV interactive effects on WM microstructure may not mean they are not in fact present. Regional mean diffusion metric measurements only allow for inference about WM microstructure across entire WM tracts, and prior DTI studies typically investigated mean-level diffusion metrics acquired from large WM tracts or WM regions of interest. As HIV-associated neurologic damage can occur well before overt cognitive manifestations emerge (as has been demonstrated in healthily-aging individuals prior to converting to mild cognitive impairment [MCI] (Whitwell et al., 2007), as well as MCI prior to conversion to

Alzheimer's disease (Ciarmiello et al., 2006), Parkinson's disease (Whitwell et al., 2007), and Huntington's disease (Horvath & Levine, 2015)), and as the pattern of HIV-related neuronal loss is not uniform, computing diffusivity metrics for a particular WM tract may be sub-optimal for capturing early changes. Therefore, coupled with the current findings, prior failures to detect interactive effects may indeed be related to cohort effects (O'Connor et al., 2017) and insufficient spatial sensitivity of the analytic methods used. *autoMATE* analyses allow for inferences about different mechanisms of WM microstructure insult that are highly spatially specific and suggest different forms of pathologic neuronal changes. Some of these WM alterations (discussed below) may account for part of the heterogeneity of cognitive impairments seen in HIV-associated neurocognitive disorders, and future investigations should focus their efforts on elucidating the neurocognitive associations with these regional WM effects. It may similarly be meaningful for future investigations to assess the effect of treatment history, including such variables as treatment initiated in the pre- versus post-HAART era as well as types of antiretroviral medications and their CNS penetrance effectiveness, on the effect of HIV and aging on WM integrity.

Further, these findings are in line with recent machine learning studies (Cole, Caan, et al., 2018; Cole, Ritchie, et al., 2018; Kuhn et al., 2018), as well as a histology study that employed a DNA-methylation technique to demonstrate a 0.1–9.3-year effective age increase in

TABLE 4 Interactive effects of HIV and age on white matter microstructure diffusivity values

Tract	FA–	MD+	AD+	RD+
CC-FRN	2.36	5.94	5.96	1.46
CC-OCC	3.96	6.13	6.54	6.31
CC-PAR	7.08	7.15	3	12.88
CC-POCG	2.77	2.73	5.96	5.33
CC-PRCG	1.79	2.42	3.98	1.97
CC-TEM	7.94	11.94	12.85	8.76
FNX	4.09	2.55	2.28	6.94
L-ARC	2.83	4.7	10.04	4.73
L-ATR	2.52	2.77	5.83	0.31
L-CGC	3.15	5.84	6.08	1.75
L-CST	9.78	7.03	3.19	1.96
L-IFO	2.85	4.64	5.31	6.68
L-ILF	1.43	3.22	7.4	4.66
R-ATR	2.57	2.06	3.18	1.1
R-CGC	5.06	12.62	4.81	19.72
R-CST	10.34	6.28	2.67	2.16
R-IFO	4.3	11.1	7.26	6.45
R-ILF	5.75	10.43	7.97	6.47

Values represent percent of entire tract where Age*HIV interaction effects were statistically significant after multiple comparison correction (FDR; $q < 0.05$). TOIs investigated: the bilateral anterior thalamic radiation (ATR), bilateral corticospinal tract (CST), bilateral inferior fronto-occipital fasciculi (IFO), bilateral inferior longitudinal fasciculus (ILF), fornix (FNX), bilateral cingulate bundle (CGC), left arcuate fasciculus (ARC), and corpus callosum (CC) fibers projecting to postcentral gyrus (CC-POC), precentral gyrus (CC-PRC), frontal lobe (CC-FRN), parietal lobe (CC-PAR), temporal lobe (CC-TEM), and occipital lobe (CC-OCC).

brain tissue in HIV+ participants (Nir et al., 2014). This accelerated aging process was hypothesized to occur via similar cellular mechanisms to those of neural aging (Jin et al., 2017). Thus, some of the pathology driving our findings may reflect an acceleration of otherwise normal, age-related processes (in line with our findings and those from the prior literature (Cole, Ritchie, et al., 2018; Gongvatana et al., 2011; Gunning-Dixon et al., 2009; McWhinney et al., 2016; Sexton et al., 2014; Westlye et al., 2010)). Such age-related mechanisms may include increased microglial proliferation with age (Von Bernhardi, Tichauer, & Eugenín, 2010), altered neuroprotective and inflammatory functions of microglia (Kipnis et al., 2004; Rogers et al., 2013), and inflammation-related (e.g., CD4+ T lymphocyte) neurogenesis within healthy tissue (Kipnis et al., 2004; Nakanishi & Wu, 2009; Ziv et al., 2006; Wolf et al., 2009); for a detailed review, see Schwartz, Kipnis, Rivest, and Prat (2013).

The current study has some limitations that should be noted. Generalizability to other ethnic groups and women is limited due to a relatively small sample consisting primarily of African-American and Caucasian males. Given the cross-sectional nature of this study, we are unable to make inferences regarding long-term outcomes or the rates of changes in WM microstructure in HIV+ individuals. Further,

the average age of our HIV+ cohort was approximately 50 years, which could be considered relatively young for studies of aging (Rickabaugh et al., 2015). Even so, although cohort effects have clearly resulted in varied results throughout the literature, our cohort age range was wide, including HIV+ participants from 24 to 76 years old and HIV– participants ages 21–66 years old, and all participants were cognitively unimpaired. As recent studies suggest that HIV infection is associated with accelerated biological aging (Hua, Schindler, McQuail, Forbes, & Riddle, 2012), and our cohort does include a relatively older HIV+ sample, it is not surprising that we were able to find main effects of age in addition to the significant interactive effect of age and HIV serostatus. Further, while reliably reported in the HIV literature, it is important to note that although the current CD4+ and viral load data used in this study were extracted from blood samples collected during the course of this study, nadir CD4+ and highest lifetime viral load were self-reported by participants. Finally, the results of *autoMATE* analyses must be interpreted with some caution, as changes in diffusion are indirect measures of WM microstructure and therefore do not give direct information on changes occurring at the cellular level. In this vein, although the *autoMATE* model took into account correlations between points within fibers in each TOI, it did not take into account correlations between fibers within each TOI or between each of the TOIs. Future models may want to consider the relationship between fibers and between TOIs as they relate to differential and joint effects of HIV and aging.

Despite these limitations, the current study provides a unique contribution to the existing literature on HIV and aging and has important potential clinical implications for neurobehavioral outcomes. As this study found that age and HIV infection conferred additional deleterious effects on WM microstructure beyond the independent effects of these factors, it is likely that older HIV+ individuals are at increased risk for cognitive problems in functions associated with these WM pathways as well as an accelerated trajectory of cognitive and functional decline. These findings indicate that providers may wish to more aggressively target modifiable risk factors for WM insult (e.g., vascular risk factors, HCV, and smoking) among HIV+ older adults to help reduce the deleterious interactive effects of older age and HIV on cognitive and functional abilities.

ACKNOWLEDGMENT

This work was supported by the University of California, Los Angeles Neurobehavioral, Neurocognitive and Functional Consequences of HIV K23 MH095661 (awarded to A.D.T.) and the Clinical and Translational Research Center Grants UL1RR033176 and UL1TR000124 (awarded to A.D.T.). K. T. and J. J. are supported by an NIH T32 Training Grant (MH19535). T.N., N.J., and P.M.T. are also supported in part by NIH grants U54EB20403 and RF1 AG041915. Y.K. and D.S. are supported in part by NIH grant R01 NS074980.

CONFLICT OF INTEREST

The authors report no conflict of interest.

PREVIOUS PRESENTATION OF THE ENCLOSED INFORMATION:

Preliminary findings similar to those reported herein and specific to the corpus callosum were presented as a poster at the 2017 meeting for the Organization for Human Brain Mapping. The citation is below:

- Kuhn, T., Jin, Y., Huang, C., Kim, Y., Nir, T.M., Gullett, J.M., Jones, J., Singer, E.J., Shattuck, D., Jahanshad, N., Bookheimer, S.Y., Hinkin, C.H., Zhu, H., Thompson, P.M., Thames, A.D. The Joint Effect of Aging and HIV Infection on Integrity of the Corpus Callosum. Twenty-third annual meeting of the Organization for Human Brain Mapping, Vancouver, British Columbia, Canada.

ORCID

Taylor Kuhn  <https://orcid.org/0000-0002-5932-1584>

REFERENCES

- Antinori, A., Arendt, G., Becker, J. T., Brew, B. J., Byrd, D. A., Cherner, M., ... Gisslen, M. (2007). Updated research nosology for HIV-associated neurocognitive disorders. *Neurology*, *69*(18), 1789–1799.
- Benjamini, Y., & Hochberg, Y. (1995). Controlling the false discovery rate: A practical and powerful approach to multiple testing. *Journal of the Royal Statistical Society. Series B (Methodological)*, *57*, 289–300.
- Bhushan, C., Haldar, J. P., Choi, S., Joshi, A. A., Shattuck, D. W., & Leahy, R. M. (2015). Co-registration and distortion correction of diffusion and anatomical images based on inverse contrast normalization. *NeuroImage*, *115*, 269–280.
- Chang, L., Andres, M., Sadino, J., Jiang, C. S., Nakama, H., Miller, E., & Ernst, T. (2011). Impact of apolipoprotein E ϵ 4 and HIV on cognition and brain atrophy: Antagonistic pleiotropy and premature brain aging. *NeuroImage*, *58*(4), 1017–1027.
- Chang, L., Wong, V., Nakama, H., Watters, M., Ramones, D., Miller, E. N., ... Ernst, T. (2008). Greater than age-related changes in brain diffusion of HIV patients after 1 year. *Journal of Neuroimmune Pharmacology*, *3*(4), 265–274.
- Ciarmiello, A., Cannella, M., Lastoria, S., Simonelli, M., Frati, L., Rubinsztein, D. C., & Squitieri, F. (2006). Brain white-matter volume loss and glucose hypometabolism precede the clinical symptoms of Huntington's disease. *Journal of Nuclear Medicine*, *47*(2), 215–222.
- Cole, J. H., Caan, M. W., Underwood, J., De Francesco, D., van Zoest, R. A., Wit, F. W., ... Majoie, C. B. (2018). No evidence for accelerated ageing-related brain pathology in treated HIV: Longitudinal neuroimaging results from the comorbidity in relation to AIDS (COBRA) project. *Clinical Infectious Diseases*, *66*, 1899–1909.
- Cole, J. H., Ritchie, S. J., Bastin, M. E., Hernández, M. V., Maniega, S. M., Royle, N., ... Wray, N. R. (2018). Brain age predicts mortality. *Molecular Psychiatry*, *23*, 1385–1392.
- Cysique, L. A., Moffat, K., Moore, D. M., Lane, T. A., Davies, N. W., Carr, A., ... Rae, C. (2013). HIV, vascular and aging injuries in the brain of clinically stable HIV-infected adults: A (1) H MRS study. *PLoS One*, *8*(4), e61738.
- Daianu, M., Mendez, M. F., Baboyan, V. G., Jin, Y., Melrose, R. J., Jimenez, E. E., & Thompson, P. M. (2016). An advanced white matter tract analysis in frontotemporal dementia and early-onset Alzheimer's disease. *Brain Imaging and Behavior*, *10*(4), 1038–1053.
- Doshi, J., Erus, G., Ou, Y., Resnick, S. M., Gur, R. C., Gur, R. E., ... Alzheimer's Neuroimaging Initiative. (2016). MUSE: MUlti-atlas region segmentation utilizing ensembles of registration algorithms and parameters, and locally optimal atlas selection. *NeuroImage*, *127*, 186–195.
- Ernst, T., & Chang, L. (2004). Effect of aging on brain metabolism in antiretroviral-naïve HIV patients. *Aids*, *18*, 61–67.
- Erus, G., Doshi, J., An, Y., Verganelakis, D., Resnick, S. M., & Davatzikos, C. (2018). Longitudinally and inter-site consistent multi-atlas based parcellation of brain anatomy using harmonized atlases. *NeuroImage*, *166*, 71–78.
- Ettenhofer, M. L., & Abeles, N. (2009). The significance of mild traumatic brain injury to cognition and self-reported symptoms in long-term recovery from injury. *Journal of Clinical and Experimental Neuropsychology*, *31*(3), 363–372.
- Filippi, C. G., Uluğ, A. M., Ryan, E., Ferrando, S. J., & van Gorp, W. (2001). Diffusion tensor imaging of patients with HIV and normal-appearing white matter on MR images of the brain. *American Journal of Neuroradiology*, *22*(2), 277–283.
- First, M. B., Spitzer, R. L., Gibbon, M., & Williams, J. B. (1997). Structured clinical interview for DSM-IV clinical version (SCID-I/CV).
- Gongvatana, A., Cohen, R. A., Correia, S., Devlin, K. N., Miles, J., Kang, H., ... Tashima, K. T. (2011). Clinical contributors to cerebral white matter integrity in HIV-infected individuals. *Journal of Neurovirology*, *17*(5), 477–486.
- Gullett, J. M., Lamb, D. G., Porges, E., Woods, A. J., Rieke, J., Thompson, P., ... Cohen, R. A. (2018). The impact of alcohol use on frontal white matter in HIV. *Alcoholism: Clinical and Experimental Research*, *42*(9), 1640–1649.
- Gunning-Dixon, F. M., Brickman, A. M., Cheng, J. C., & Alexopoulos, G. S. (2009). Aging of cerebral white matter: A review of MRI findings. *International Journal of Geriatric Psychiatry*, *24*(2), 109–117.
- Harezlak, J., Buchthal, S., Taylor, M., Schifitto, G., Zhong, J., Daar, E., ... Navia, B. (2011). HIV neuroimaging consortium: Persistence of HIV-associated cognitive impairment, inflammation, and neuronal injury in era of highly active antiretroviral treatment. *Aids*, *25*, 625–633.
- Heaton, R. K., Clifford, D. B., Franklin, D. R., Woods, S. P., Ake, C., Vaida, F., ... Rivera-Mindt, M. (2010). HIV-associated neurocognitive disorders persist in the era of potent antiretroviral therapy CHARTER study. *Neurology*, *75*(23), 2087–2096.
- Hinkin, C. H., Castellon, S. A., Atkinson, J. H., & Goodkin, K. (2001). Neuropsychiatric aspects of HIV infection among older adults. *Journal of Clinical Epidemiology*, *54*(12), S44–S52.
- Holt, J. L., Kraft-Terry, S. D., & Chang, L. (2012). Neuroimaging studies of the aging HIV-1-infected brain. *Journal of Neurovirology*, *18*(4), 291–302.
- Horvath, S., & Levine, A. J. (2015). HIV-1 infection accelerates age according to the epigenetic clock. *The Journal of Infectious Diseases*, *212*(10), 1563–1573.
- Hua, K., Schindler, M. K., McQuail, J. A., Forbes, M. E., & Riddle, D. R. (2012). Regionally distinct responses of microglia and glial progenitor cells to whole brain irradiation in adult and aging rats. *PLoS One*, *7*(12), e52728.
- Jin, Y., Huang, C., Daianu, M., Zhan, L., Dennis, E. L., Reid, R. I., ... Thompson, P. M. (2017). 3D tract-specific local and global analysis of white matter integrity in Alzheimer's disease. *Human Brain Mapping*, *38*(3), 1191–1207.
- Jin, Y., Shi, Y., Zhan, L., Gutman, B. A., de Zubicaray, G. I., McMahon, K. L., ... Thompson, P. M. (2014). Automatic clustering of white matter fibers in brain diffusion MRI with an application to genetics. *NeuroImage*, *100*, 75–90.
- Jin, Y., Shi, Y., Zhan, L., & Thompson, P. M. (2015, April). Automated multi-atlas labeling of the fornix and its integrity in Alzheimer's disease. In *Biomedical imaging (ISBI), 2015 IEEE 12th International symposium on* (pp. 140–143). IEEE.
- Joint United Nations Programme on HIV/AIDS. (2016). *Global AIDS update 2016*. Geneva: UNAIDS.

- Kipnis, J., Cardon, M., Avidan, H., Lewitus, G. M., Mordechay, S., Rolls, A., ... Schwartz, M. (2004). Dopamine, through the extracellular signal-regulated kinase pathway, downregulates CD4+ CD25+ regulatory T-cell activity: Implications for neurodegeneration. *Journal of Neuroscience*, 24(27), 6133–6143.
- Kuhn, T., Kaufmann, T., Doan, N. T., Westlye, L. T., Jones, J., Nunez, R. A., ... Thames, A. D. (2018). An augmented aging process in brain white matter in HIV. *Human Brain Mapping*, 39(6), 2532–2540.
- Kuhn, T., Schonfeld, D., Sayegh, P., Jones, J. D., Arentoft, A., Hinkin, C. H., ... Thames, A. D. (2016). The effects of HIV and aging on subcortical shape alterations: A 3D morphometric study. *Human Brain Mapping*, 38(2), 1025–1037. <https://doi.org/10.1002/hbm.23436>
- McWhinney, S. R., Tremblay, A., Chevalier, T. M., Lim, V. K., & Newman, A. J. (2016). Using CForest to analyze diffusion tensor imaging data: A study of white matter integrity in healthy aging. *Brain Connectivity*, 6(10), 747–758.
- Morgan, E. T., Lee, C. M., & Nyagode, B. A. (2011). Regulation of drug metabolizing enzymes and transporters in infection, inflammation, and cancer. *Encyclopedia of drug metabolism and interactions* (pp. 1–45).
- Mori, S., Oishi, K., Jiang, H., Jiang, L., Li, X., Akhter, K., ... Toga, A. W. (2008). Stereotaxic white matter atlas based on diffusion tensor imaging in an ICBM template. *NeuroImage*, 40(2), 570–582.
- Nakanishi, H., & Wu, Z. (2009). Microglia-aging: Roles of microglial lysosome- and mitochondria-derived reactive oxygen species in brain aging. *Behavioural Brain Research*, 201(1), 1–7.
- Nir, T. M., Jahanshad, N., Busovaca, E., Wendelken, L., Nicolas, K., Thompson, P. M., & Valcour, V. G. (2014). Mapping white matter integrity in elderly people with HIV. *Human Brain Mapping*, 35(3), 975–992.
- O'Connor, E. E., Jaillard, A., Renard, F., & Zeffiro, T. A. (2017). Reliability of white matter microstructural changes in HIV infection: Meta-analysis and confirmation. *American Journal of Neuroradiology*, 38(8), 1510–1519.
- Pomara, N., Crandall, D. T., Choi, S. J., Johnson, G., & Lim, K. O. (2001). White matter abnormalities in HIV-1 infection: a diffusion tensor imaging study. *Psychiatry Research: Neuroimaging*, 106(1), 15–24.
- Price, R., Bartlett, J., & Bloom, A. (2016). HIV-associated neurocognitive disorders: Epidemiology, clinical manifestations, and diagnosis. (pp. 2–22).
- Rickabaugh, T. M., Baxter, R. M., Sehl, M., Sinsheimer, J. S., Hultin, P. M., Hultin, L. E., ... Jamieson, B. D. (2015). Acceleration of age-associated methylation patterns in HIV-1-infected adults. *PLoS One*, 10(3), e0119201.
- Rogers, N., Cheah, P. S., Szarek, E., Banerjee, K., Schwartz, J., & Thomas, P. (2013). Expression of the murine transcription factor SOX3 during embryonic and adult neurogenesis. *Gene Expression Patterns*, 13(7), 240–248.a.
- Sacktor, N., Skolasky, R. L., Cox, C., Selnes, O., Becker, J. T., Cohen, B., ... Miller, E. N. (2010). Longitudinal psychomotor speed performance in human immunodeficiency virus-seropositive individuals: Impact of age and serostatus. *Journal of Neurovirology*, 16(5), 335–341.
- Schwartz, M., Kipnis, J., Rivest, S., & Prat, A. (2013). How do immune cells support and shape the brain in health, disease, and aging? *Journal of Neuroscience*, 33(45), 17587–17596.
- Schwartzman, A., Dougherty, R. F., Lee, J., Ghahremani, D., & Taylor, J. E. (2009). Empirical null and false discovery rate analysis in neuroimaging. *NeuroImage*, 44(1), 71–82.
- Seider, T. R., Gongvatana, A., Woods, A. J., Chen, H., Porges, E. C., Cummings, T., ... Cohen, R. A. (2016). Age exacerbates HIV-associated white matter abnormalities. *Journal of Neurovirology*, 22(2), 201–212.
- Sexton, C. E., Walhovd, K. B., Storsve, A. B., Tamnes, C. K., Westlye, L. T., Johansen-Berg, H., & Fjell, A. M. (2014). Accelerated changes in white matter microstructure during aging: A longitudinal diffusion tensor imaging study. *Journal of Neuroscience*, 34(46), 15425–15436.
- Shattuck, D. W., Sandor-Leahy, S. R., Schaper, K. A., Rottenberg, D. A., & Leahy, R. M. (2001). Magnetic resonance image tissue classification using a partial volume model. *NeuroImage*, 13(5), 856–876.
- Smith, S. M., Jenkinson, M., Woolrich, M. W., Beckmann, C. F., Behrens, T. E., Johansen-Berg, H., ... Niazy, R. K. (2004). Advances in functional and structural MR image analysis and implementation as FSL. *NeuroImage*, 23, S208–S219.
- Summers, Mathew J., and Mark W. Bondi (2017). Editorial introduction to the special issue on neuropsychological assessment in aging. (pp. 303–304).
- Towgood, K. J., Pitkanen, M., Kulasegaram, R., Fradera, A., Kumar, A., Soni, S., ... Kopelman, M. D. (2012). Mapping the brain in younger and older asymptomatic HIV-1 men: Frontal volume changes in the absence of other cortical or diffusion tensor abnormalities. *Cortex*, 48(2), 230–241.
- Valcour, V., Shikuma, C., Shiramizu, B., Watters, M., Poff, P., Selnes, O., ... Sacktor, N. (2004a). Higher frequency of dementia in older HIV-1 individuals the Hawaii aging with HIV-1 cohort. *Neurology*, 63(5), 822–827.
- Valcour, V., Sithinamsuwan, P., Letendre, S., & Ances, B. (2011). Pathogenesis of HIV in the central nervous system. *Current HIV/AIDS Reports*, 8(1), 54–61.
- Vance, D. E., McGuinness, T., Musgrove, K., Orel, N. A., & Fazeli, P. L. (2011). Successful aging and the epidemiology of HIV. *Clinical Interventions in Aging*, 6, 181.
- Von Bernhard, R., Tichauer, J. E., & Eugenin, J. (2010). Aging-dependent changes of microglial cells and their relevance for neurodegenerative disorders. *Journal of Neurochemistry*, 112(5), 1099–1114.
- Wang, Y., Wang, Q., Haldar, J. P., Yeh, F. C., Xie, M., Sun, P., ... Song, S. K. (2011). Quantification of increased cellularity during inflammatory demyelination. *Brain*, 134(12), 3590–3601.
- Westlye, L. T., Walhovd, K. B., Dale, A. M., Bjørnerud, A., Due-Tønnessen, P., Engvig, A., ... Fjell, A. M. (2010). Differentiating maturational and aging-related changes of the cerebral cortex by use of thickness and signal intensity. *NeuroImage*, 52(1), 172–185.
- Whitwell, J. L., Przybelski, S. A., Weigand, S. D., Knopman, D. S., Boeve, B. F., Petersen, R. C., & Jack, C. R., Jr. (2007). 3D maps from multiple MRI illustrate changing atrophy patterns as subjects progress from mild cognitive impairment to Alzheimer's disease. *Brain*, 130(7), 1777–1786.
- Wolf, S. A., Steiner, B., Akpinarli, A., Kammertoens, T., Nassenstein, C., Braun, A., ... Kempermann, G. (2009). CD4-positive T lymphocytes provide a neuroimmunological link in the control of adult hippocampal neurogenesis. *The Journal of Immunology*, 182(7), 3979–3984.
- Wright, P., Heaps, J., Shimony, J. S., Thomas, J. B., & Ances, B. M. (2012). The effects of HIV and combination antiretroviral therapy on white matter integrity. *AIDS (London, England)*, 26(12), 1501.
- Wu, Y., Storey, P., Cohen, B. A., Epstein, L. G., Edelman, R. R., & Ragin, A. B. (2006). Diffusion alterations in corpus callosum of patients with HIV. *American Journal of Neuroradiology*, 27(3), 656–660.
- Zhu, H., Kong, L., Li, R., Styner, M., Gerig, G., Lin, W., & Gilmore, J. H. (2011). FADTTS: Functional analysis of diffusion tensor tract statistics. *NeuroImage*, 56, 1412–1425.
- Ziv, Y., Ron, N., Butovsky, O., Landa, G., Sudai, E., Greenberg, N., ... Schwartz, M. (2006). Immune cells contribute to the maintenance of neurogenesis and spatial learning abilities in adulthood. *Nature Neuroscience*, 9(2), 268–275.

How to cite this article: Kuhn T, Jin Y, Huang C, et al. The joint effect of aging and HIV infection on microstructure of white matter bundles. *Hum Brain Mapp*. 2019;40:4370–4380. <https://doi.org/10.1002/hbm.24708>